Proceedings the 44th International School and Conference on the Physics of Semiconductors "Jaszowiec 2015", Wisła 2015

Dynamical and Tuneable Modulation of the Tamm Plasmon/Exciton–Polariton Hybrid States Using Surface Acoustic Waves

J.V.T. Buller[a,*], E.A. Cerda-Méndez[a], R.E. Balderas-Navarro[b] and P.V. Santos[a]

[a]Paul-Drude-Institut für Festkörperelektronik, 10117 Berlin, Germany

[b]Instituto de Investigación en Comunicación Óptica-UASLP, 78000 San Luis, Mexico

In this work, we discuss theoretically the formation of the Tamm plasmon/exciton–polariton hybrid states in an (Al,Ga)As microcavity and their modulation by surface acoustic waves. The modulation of the Tamm plasmon/exciton–polariton states origins in the change of the excitonic band gap energy and the thickness change of the sample structure layers due to the induced strain fields by surface acoustic waves. The frequency f_{SAW} of the acoustic modulation of the Tamm plasmon/exciton–polariton states is limited by the thickness of the upper distributed Bragg reflector. For the Tamm plasmon/exciton–polariton states in $Al_xGa_{1-x}As/GaAs$ structures f_{SAW} is in the range of 370 MHz while f_{SAW} in GHz range is possible for the parametric Tamm plasmon/exciton–polariton states. In both cases, the acoustic modulation is several meV for typical acoustic power levels.

DOI: 10.12693/APhysPolA.129.A-26

PACS: 71.36.+c, 42.55.Sa, 85.50.–n

1. Introduction

The development of new optoelectronic devices operating at low threshold powers and at high switching frequencies is a complex and challenging task, which can only be overcome by exploiting new physical phenomena [1–4] and applying them to device implementations [5, 6]. One of such new promising physical phenomenon are exciton–polaritons in semiconductor microcavities (MCs). Exciton–polaritons are unique bosonic half-light half-matter quasiparticles that result from the strong coupling between the photonic mode of a MC and quantum well (QW) excitons embedded in the active MC region (*cf.* Fig. 1a, [7]). The inter-excitonic interactions between polaritons give rise to optical nonlinearities several orders of magnitude higher than in purely photonic systems. Due to the photonic component polaritons have a very low effective mass (10^{-5}–10^{-4} mass of a free electron) leading to a de Broglie wavelength λ_{dB} of a few μm and thus to the possibility to form macroscopic coherent quantum phases at low densities and at elevated temperatures (on the order of a few K) as well as to be manipulated by micro-scale potentials [8, 9]. Various polariton-based device concepts, like polariton-based transistors and logic gates, as well as their implementation in quantum information processing have been proposed [10, 11].

The fabrication of polaritonic devices requires reliable and practical potentials for controlling, confining and guiding exciton-polaritons in MC structure. One interesting option is provided by dynamic strain potentials [12] induced by a surface acoustic wave (SAW) [13, 14]. SAWs are mechanical vibrations propagating along a surface (*cf.* Fig. 1c): the strain field of a SAW with wavelength λ_{SAW} smaller than λ_{dB} creates a tuneable acoustic lattice for the control of the polariton properties. Since the SAW penetration depth is comparable to λ_{SAW}, an efficient acoustic modulation requires that λ_{SAW} is larger than the thickness of the upper MC distributed Bragg reflector (DBR). In this contribution, we demonstrate that this limitation can be overcome by exploiting plasmonic resonances induced by thin metallic stripes deposited on the top of the MC structure. In this case, new quasiparticles called the Tamm plasmon/exciton–polaritons (TPEP) form by the superposition of the Tamm plasmons (TPs) at the metal-semiconductor interface and the exciton–polaritons in the MC [10]. The aim of this work is to explore the dynamical and tuneable modulation of TPEP modes by SAW at frequencies close to and in the gigahertz range.

2. Sample design

The proposed sample structure supporting TPEP states consists of a gold layer on top of a DBR consisting of $Al_xGa_{1-x}As$ layers with a thickness $\lambda/(4n_i)$ (i = $Al_{15}Ga_{85}As$, $Al_{80}Ga_{20}As$), where n_i is the refractive index and λ the MC resonance wavelength (cf. Fig. 1a). The structure supports TP modes at the metal–semiconductor interface only when the DBR layer adjacent to the metal has a higher refractive index than its following DBR layer [16]. The energy E_{T} of the TP mode can be tuned by changing the thickness of the metal and/or of the adjacent DBR layer. When E_{T} is in resonance with the MC mode and the QW exciton energy, the resulting coupled system can be described using the three level coupled oscillator model given by

*corresponding author; e-mail: buller@pdi-berlin.de

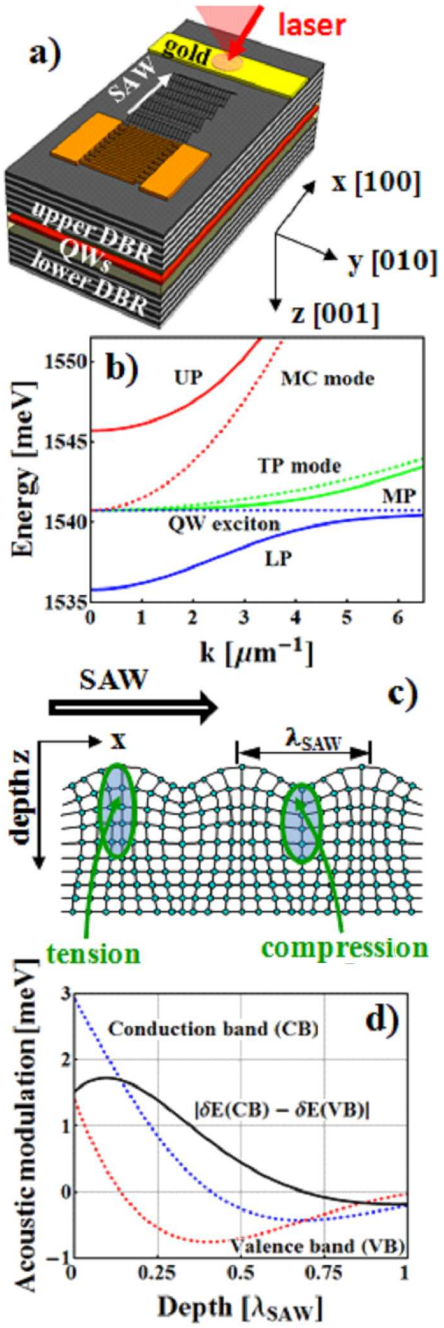

Fig. 1. (a) Schematic view of the sample structure; sample A: 50 nm gold layer, 21 upper $\lambda/4$ DBR pairs, $3\lambda/2$ cavity with 6 QWs and 50 lower $\lambda/4$ DBR pairs for formation of TPEP states, where $\lambda = 805$ nm is the MC resonance wavelength. The QW exciton energy is in resonance with the TP and the MC mode. Structure of sample B is similar to sample A differing by: 30 nm gold layer, 4 upper $\lambda/4$ DBR pairs and $\lambda = 780$ nm. (b) Dispersion of TPEP states of sample A (solid lines) where UP is the upper, MP the middle, and LP is the lower TPEP state. The dotted lines represent the dispersion of uncoupled TP mode, MC mode and QW excitons. (c) SAWs propagate on the sample surface creating regions of tension and compression, leading to a (d) depth-dependent modulation of the conduction (δE(CB)) and valence band (δE(VB)) energies.

$$\widehat{H} = \begin{pmatrix} E_{\rm T} & \frac{\Omega_{\rm T-C}}{2} & 0 \\ \frac{\Omega_{\rm T-C}}{2} & E_{\rm C} & \frac{\Omega_{\rm C-X}}{2} \\ 0 & \frac{\Omega_{\rm C-X}}{2} & E_{\rm X} \end{pmatrix}, \quad (1)$$

where $E_{\rm T}$, $E_{\rm C}$ and $E_{\rm X}$ are the uncoupled eigenenergies of the TP mode, the MC mode and the QW excitons, respectively. The solution of $\widehat{H}|\Psi\rangle = E|\Psi\rangle$ yields the eigenstates and -energies of the TPEP modes which are the linear combinations of the TP mode $|T\rangle$, MC mode $|C\rangle$ and QW exciton $|X\rangle$, $|\Psi\rangle = \alpha|T\rangle + \beta|C\rangle + \gamma|X\rangle$. α, β and γ are the corresponding Hopfield coefficients.

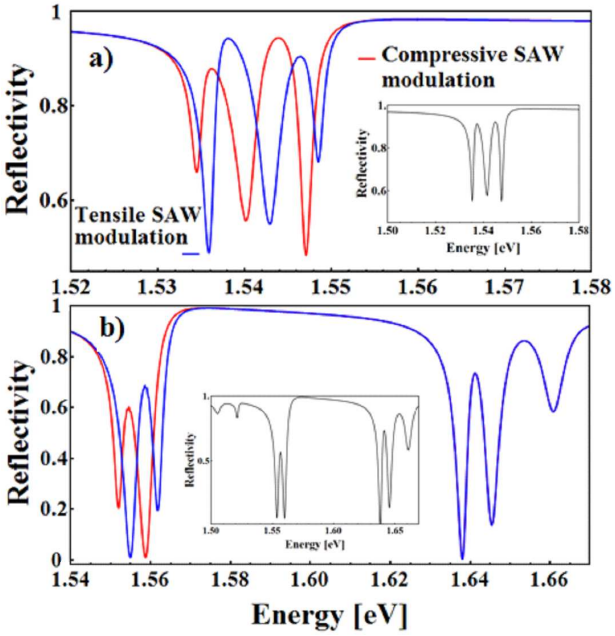

Fig. 2. Calculated reflectivity spectra under acoustic modulation introduced by SAW with a power density $P_{\rm SAW} = 300$ W/m ($P_{\rm SAW}$ is the SAW power per unit length perpendicular to the propagation direction). The insets show the calculated reflectivity spectra without acoustic modulation. (a) Acoustic modulation of sample A (*cf.* Fig. 1) at $f_{\rm SAW} = 370$ MHz and (b) of sample B (*cf.* Fig. 1) at $f_{\rm SAW} = 1.4$ GHz. The reflectivity dips above 1.64 eV represent the DBR stop band. There is no modulation of the upper TPEP state at 1.637 eV.

The coupling strengths between the TP state and the MC mode ($\Omega_{\rm T-C}$) and between the MC mode and the QW excitons ($\Omega_{\rm C-X}$) determine, besides the Rabi splitting, the mixing of these states in the TPEP modes. $\Omega_{\rm T-C}$ is given by $\Omega_{\rm T-C} \approx \frac{\sqrt{2}(n_{\rm B}/n_{\rm A})^N (n_{\rm A}-n_{\rm B})}{\pi\sqrt{n_{\rm A}(2n_{\rm A}-n_{\rm B})}}\hbar\omega_{\rm DBR}$ and decreases exponentially with the number N of the upper DBR layers [15]. $\Omega_{\rm C-X}$ is well approximated by $\Omega_{\rm C-X} \approx 2\sqrt{(2\Gamma_{\rm X} cN)/(n_{\rm C} L_{\rm eff})}\hbar$: it depends on the exciton radiative decay rate $\Gamma_{\rm X}$, the speed of light c, the effective MC refractive index $n_{\rm C}$ and the effective MC length $L_{\rm eff}$ [7]. We neglected in Eq. (1) the direct coupling between excitons and TP states.

When all states are in resonance and $\Omega_{\mathrm{C-X}} = \Omega_{\mathrm{T-C}}$, then $\alpha = \beta = \gamma$. For the $Al_xGa_{1-x}As$/GaAs structures (*cf.* Fig. 1a), this can only be achieved by using a relatively thick upper DBR (21 pairs of $\lambda/4$ layers) to ensure that $\Omega_{\mathrm{T-C}} \sim \Omega_{\mathrm{C-X}}$. $\Omega_{\mathrm{C-X}}$ is assumed to be 6 meV. Figure 1b shows the in-plane polariton dispersion of a sample satisfying this condition (sample A, layer structure described in the caption of Fig. 1). The inset of Fig. 2a shows the calculated reflectivity spectrum of the TPEP states for the same sample using a transfer matrix method. The linewidth of the TPEP states is 2.5 meV and is limited by the absorption of the gold layer and its finite reflectivity. The Rabi splitting between lower and upper TPEP mode is 12 meV and 6 meV between the lower/upper and middle TPEP mode.

As will be discussed in the following section, sample A has a relatively thick upper DBR and requires a large λ_{SAW} for efficient acoustic modulation of TPEP states. To achieve modulation by SAWs at gigahertz frequencies, we propose another sample structure with reduced number of upper DBR pairs and reduced gold layer thickness. In this sample (sample B described in the caption of Fig. 1) the TP and the MC mode are tuned to be in resonance and the QW excitons are shifted by $-\Omega_{\mathrm{T-C}}/2$ with respect to the TP and MC mode resonance energy. TP and MC mode couple to the upper and lower optical branches with the Rabi splitting determined by $\Omega_{\mathrm{T-C}}$. The lower branch can couple to the QW excitons. This results in the formation of exciton–polariton states mediated by strongly optically coupled TP and MC modes which can be seen as parametric TPEP modes. The advantage of the sample B over sample A is the bigger Rabi splitting $\Omega_{\mathrm{T-C}}$, reduced light absorption by the gold layer and the possibility of applying SAWs at gigahertz frequencies for the modulation of the TPEP modes.

3. Acoustic modulation

SAW can be generated using interdigital transducers (IDTs) as illustrated in Fig. 1a. The SAW frequency f_{SAW} is given by $f_{\mathrm{SAW}} = v_{\mathrm{SAW}}/\lambda_{\mathrm{SAW}}$ where v_{SAW} is the SAW velocity ($v_{\mathrm{SAW}} = 3$ μm/ns in GaAs) [17]. The SAW creates in the sample regions of tension and compression (Fig. 1c). The related deformation potential modulates the valence band (VB) energy E_{VB} and the conduction band (CB) energy E_{CB} and thus, the energy band gap E_{g} of the QW excitons which is $E_{\mathrm{g}} = E_{\mathrm{CB}} - E_{\mathrm{VB}}$. The shifts of the CB and/or VB energy are given by $\Delta E_{\mathrm{CB}} = a_{\mathrm{CB}} S_0$ and $\Delta E_{\mathrm{VB}} = a_{\mathrm{VB}} S_0 \pm b_{\mathrm{VB}} (S_{zz} - \frac{S_{xx}}{2})$, where a_{CB} and a_{VB} are the hydrostatic CB and VB deformation potentials, respectively, and b_{VB} is the uniaxial deformation potential. S_0 is the hydrostatic strain related to the SAW induced volume change and S_{xx} and S_{zz} are the strain fields into the propagation direction x and the penetration depth z of the SAW [18]. The sign $\pm$ refers to hh and lh states of the QW exciton

$$\Delta E_{\mathrm{g}} = (a_{\mathrm{CB}} + a_{\mathrm{VB}})\, S_0 \pm b_{\mathrm{VB}} \left(S_{zz} - \frac{S_{xx}}{2} \right). \qquad (2)$$

Figure 1d displays numerical calculations for the acoustic modulation of VB and CB for a pure GaAs system which is a good approximation for the proposed samples A and B. QW excitons experience maximal acoustic modulation of the band gap energy at the depth of approximately $\frac{1}{4}\lambda_{\mathrm{SAW}}$ where ΔE_{VB} and ΔE_{CB} have opposite signs. The position of the QWs in the sample structure defines the wavelength λ_{SAW} of the SAW for the maximal acoustic modulation of TPEP states. In case of sample A with 21 upper $\lambda/4$ DBR pairs, QWs are positioned at 2 μm yielding $\lambda_{\mathrm{SAW}} = 8$ μm and $f_{\mathrm{SAW}} = 370$ MHz. The corresponding maximal acoustic modulation ΔE_{g} is calculated to be ± 2.5 meV for the linear SAW power density $P_{\mathrm{SAW}} = 300$ W/m.

Additionally to the modulation of the QW exciton energy E_{g}, SAWs modulate the thickness of the sample layers and thus, the density of the layers and their refractive indices. The latter results in the modulation of the MC mode energy E_{C} by ΔE_{C} and the TP energy E_{T} by ΔE_{T}, where $\Delta E_{\mathrm{C}} \approx \frac{1}{4}\Delta E_{\mathrm{g}}$ and ΔE_{T} in order of a few 0.1 meV. The total acoustic modulation of the TPEP states is displayed in Fig. 2a. The modulation of the intensity and the energy of the TPEP modes is expected to be observable. The acoustic modulation could be further increased by increasing the gold layer thickness (not shown). The latter results in the higher absorption of light by the gold layer. A compromise is found for a gold layer thickness of 50 nm.

Figure 2b displays the acoustic modulation of TPEP states for a sample B at SAW frequency of 1.4 GHz. Since $\Delta E_{\mathrm{g}} \ll \Omega_{\mathrm{T-C}}$ ($\Delta E_{\mathrm{g}} = \pm 3$ meV and $\Omega_{\mathrm{T-C}} \approx 80$ meV), the acoustic modulation mainly influences the lower and middle TPEP states where the modulation of the excitonic component is of the same order of magnitude as the Rabi splitting, $\Delta E_{\mathrm{g}} \sim \Omega_{\mathrm{C-X}}$. The acoustic modulation is bigger than the linewidth of the TPEP modes which is 4 meV.

4. Conclusion

We proposed a sample structure supporting the formation of TPEP states and their modulation by SAWs at $f_{\mathrm{SAW}} = 370$ MHz by ± 3 meV (sample A). The acoustic modulation at gigahertz frequencies is possible by positioning the QWs close to the sample surface (sample B). Here, parametric TPEP states form with $\Omega_{\mathrm{T-C}} \approx 80$ meV where mainly the lower and middle TPEP states are modulated by SAWs at $f_{\mathrm{SAW}} = 1.4$ GHz by ± 4 meV. The results open the way towards feasible signal modulation in polaritonic devices as well as towards trapping of exciton–polaritons at single particle level.

Acknowledgments

The authors wish to thank T. Flissikowski for fruitful discussions. This work was supported by DFG Grant No. CE 191/2-1.

References

[1] L. Novotny, B. Hecht, *Principles of Nano-Optics*, Cambridge University Press, New York 2006.

[2] J. Kasprzak, M. Richard, S. Kundermann, A. Baas, P. Jeambrun, J.M.J. Keeling, F.M. Marchetti, M.H. Szymańska, R. André, J.L. Staehli, V. Savona, P.B. Littlewood, B. Deveaud, Le Si Dang, *Nature (London)* **443**, 409 (2006).

[3] A. Amo, J. Lefrère, S. Pigeon, C. Adrados, C. Ciuti, I. Carusotto, R. Houdré, E. Giacobino, A. Bramati, *Nature Phys.* **5**, 805 (2009).

[4] K.G. Lagoudaki, M. Wouters, M. Richard, A. Baas, I. Carusotto, R. André, Le Si Dang, B. Deveaud-Plédran, *Nature Phys.* **4**, 706 (2008).

[5] S. Maier, *Plasmonics: Fundamentals and Applications*, Springer, New York 2007.

[6] T.C.H. Liew, A.V. Kavokin, T. Ostatnický, M. Kaliteevski, I.A. Shelykh, R.A. Abram, *Phys. Rev. B* **82**, 033302 (2010).

[7] A. Kavokin, J.J. Baumberg, G. Malpuech, F.P. Laussy, *Microcavities*, Oxford University Press, New York 2007.

[8] C.W. Lai, N.Y. Kim, S. Utsunomiya, G. Roumpos, H. Deng, M.D. Fraser, T. Byrnes, P. Recher, N. Kumada, T. Fujisawa, Y. Yamamoto, *Nature (London)* **450**, 529 (2007).

[9] D. Tanese, H. Flayac, D. Solnyshkov, A. Amo, A. Lemaître, E. Galopin, R. Braive, P. Senellart, I. Sagnes, G. Malpuech, J. Bloch, *Nature Commun.* **4**, 1749 (2013).

[10] D. Ballarini, M. De Giorgi, E. Cancellieri, R. Houdré, E. Giacobino, R. Cingolani, A. Bramati, G. Gigli, D. Sanvitto, *Nature Commun.* **4**, 1778 (2013).

[11] I.M. Georgescu, S. Ashhab, F. Nori, *Rev. Mod. Phys.* **86**, 153 (2014).

[12] Xue Ben, H.S. Park, *Appl. Phys. Lett.* **102**, 041909 (2013).

[13] E.A. Cerda-Méndez, D.N. Krizhanovskii, M. Wouters, R. Bradley, K. Biermann, K. Guda, R. Hey, P.V. Santos, D. Sarkar, M.S. Skolnick, *Phys. Rev. Lett.* **105**, 116402 (2010).

[14] E.A. Cerda-Méndez, D. Sarkar, D.N. Krizhanovskii, S.S. Gavrilov, K. Biermann, M.S. Skolnick, P.V. Santos, *Phys. Rev. Lett.* **111**, 146401 (2013).

[15] M. Kaliteevski, S. Brand, R.A. Abram, I. Iorsh, A.V. Kavokin, I.A. Shelykh, *Appl. Phys. Lett.* **95**, 251108 (2009).

[16] M. Kaliteevski, I. Iorsh, S. Brand, R.A. Abram, J.M. Chamberlain, A.V. Kavokin, I.A. Shelykh, *Phys. Rev. B* **76**, 165415 (2007).

[17] S. Adachi, *GaAs and Related Materials: Bulk Semiconducting and Superlattice Properties*, World Sci., 1994.

[18] P. Yu, M. Cardona, *Fundamentals of Semiconductors*, Springer, Berlin 2010.